Indian Journal of Engineering & Materials Sciences
Vol. 27, February 2020, pp. 104-111

# Electrochemical characterization of samples of commercial steel treated with acetylene plasma

Natal Nerímio Regone[a]*, Maria Eliziane Pires de Souza[b], Célia Marina Alvarenga Freire[c], Margarita Ballester[c], Elidiane Cipriano Rangel[d] & Nilson Cristino da Cruz[d]

[a]São Paulo State University-UNESP 13876-750, São João da Boa Vista, SP, Brasil
[b]Mechanical Engineering, Federal University of Maranhão, 65080-805, São Luís, MA, Brasil
[c]Faculty of Mechanical Engineering, University of Campinas-UNICAMP, 13083-970, Campinas, SP, Brasil
[d] São Paulo State University-UNESP, 18087-180, Sorocaba, SP, Brasil

*Received: 21 August 2018; Accepted: 6 December 2019*

Cutting tools have been employed in wood processing must be corrosion and wear resistant due to the acidic composition of wood and the wear generated during cutting, which lead to the deterioration of steel saws. Hydrogenated amorphous carbon films possess mechanical, tribological and barrier properties that can increase the hardness, wear and corrosion resistance of this type of tool. This work has involved an investigation of the effectiveness of plasma-deposited amorphous carbon thin films in protecting commercial carbon steel saws. Before deposition, the substrates were sputter-cleaned in argon plasma (19.27 Pa; 50 W) for 180 s. The films have been deposited using acetylene and argon mixtures excited by a radio frequency power supply (13.56 MHz, 70 W). The concentration of acetylene in the mixture has been varied in the inverse proportion to that of argon so as to maintain a constant total gas pressure of 1.8 Pa. The deposition time was 3600 s. The chemical behavior of the coated saws have been evaluated by electrochemical impedance spectroscopy (EIS) and polarization curves.Surface images of the plasma-coated samples have been recorded by scanning electron microscopy (SEM). The results have indicated that the plasma treatment has increased the corrosion resistance of carbon steel samples in acidic solutions.

**Keywords:** Saw, Impedance, Polarization, Plasma enhanced chemical vapor deposition (PECVD)

## 1 Introduction

The cutting edges of tools employed in wood processing lose their sharpness due to the abrasive process to which they are subjected. The presence of mineral salts, formic acid and acetic acid in wood composites deteriorates the tool by corroding its metal[1]. Therefore, the loss of edge sharpness is a process of tribo-corrosion that depends on the type of wood and the composition of the material of the saw. To extend the tool's service life and thus reduce the frequency of sharpening, the surface properties of the material of the saw must be improved. A versatile, ecologically clean, easy and economically feasible way to produce protective coatings on various types of surfaces is by plasma deposition of thin films[2–8]. This technique involves the preparation of films with controlled thicknesses onto different types of materials.

Deposition plasmas, also called luminescent glow discharges, are generated in low pressure reactors or chambers by exposing vapors of organic compounds to electrical and magnetic fields. The properties of films depend on discharge excitation parameters such as the chemical composition and pressure of the gases in the reactor, the power and frequency of the excitation signal, and the temperature of the samples during the process[9,10]. The properties of films obtained can be achieved by varying these parameters, e.g., thin insulating or conducting films for the fabrication of electronic devices[11], films for optical and biomedical applications,[12,13], and hydrophobic materials[14] for food packaging and swimming clothes.

A special class of plasma-deposited films is hydrogenated amorphous carbons,[15,16], a-C:H[17]. These materials are extremely hard and electrically resistive, chemically inert, and have a low attrition coefficient due to their structure, which is abundant in tetragonal hybridized carbon bonds[18,19]. According to previous studies, the acetylene and argon film prepared in this research work is a carbon polymer composite material constituted of hybridized $sp^2$ and $sp^3$ carbon in

*Corresponding author (E-mail: natal.regone@unesp.br)

coatings for magnetic recording tapes[20]. Several reports in the literature demonstrate the functionality of this type of material in applications such as hard coatings for cutting tools, automotive parts, microcomputer hard disks, optical windows[21–23], in bio- and hemocompatible coatings for heart valves, dental arch wire, intravenous devices for the treatment of heart diseases, bone prostheses, artificial joints[24–27] coatings for magnetic tape recording head[28].

In Pathem's study of carbon deposition for use in magnetic recording, the filtered cathodic arc deposits were found to exhibit a five-fold lower oxidation rate than that of plasma films produced by chemical deposition. Based on the $sp^3$ bonds and oxidation rate, this paper shows that there is an inherent relationship between chemical bonds and the corrosion process[29]. Hydrogenated diamond-like carbon (DLC) films as thin as 2 nm were deposited on the magnetic layer of hard drives, aiming to reduce the damage caused by interaction with the head and to optimize the distance between the head and the magnetic layer[30]. The protective layer was deposited using the *plasma-enhanced chemical vapor deposition (*PECVD)[31], technique from compounds such as $CH_4$, $C_2H_2$ and $C_2H_6$. The most relevant factors for the production of coatings with the desired properties were defined by varying the composition of the atmosphere, self-bias voltage, anode polarization, and monomer flow rate, using the ANOVA method.

In the latest researches about plasma deposition to anti-corrosive applications can be cited the works of Pillai and Moolsradoo. Pillai studied about deposition of SiC over carbon fiber through plasma enhanced chemical vapor deposition. The coating of SiC has high thermo-chemical stability. SiC film are used to corrosion protection in automotive industry, reactors, and engines[32]. Other investigation of Pillai was about deposition of $SiO_2$ over carbon fiber using radio frequency plasma enhanced chemical vapor deposition technique. The coating of $SiO_2$ showed amorphous phase of needle like nanostructures. The best condition of corrosion resistance was obtained on the deposition process of $10^{-2}$ mbar[33]. Moolsradoo reported the deposition of pure Diamond-like carbon (DLC), silicon DLC, and silicon/nitrogen DLC to measure the influence of silicon, and of silicon/carbon on corrosion resistance and hardness of the coating. The results showed that the increase of silicon concentration over the coating improve film hardness and corrosion resistance. The increase of proportion of elements silicon/nitrogen produce a reduction on hardness and corrosion resistance of this coating[34]. In this work, hydrogenated amorphous thin films were deposited on the blades of commercial carbon steel saws using acetylene/argon plasma mixtures. The corrosion resistance of the films was evaluated based on electrochemical impedance spectroscopy (EIS) and polarization spectroscopy (PS) tests. The final aspect of the surfaces exposed to the tests was evaluated by scanning electron microscopy (SEM).

## 2 Materials and Methods

Samples were prepared from commercial carbon steel saws, which are identified in this paper as types 1 and 2. The percentage composition of the chemical constituents of the samples was determined by inductively coupled plasma optical emission spectroscopy (ICP-OES). Table 1 shows the chemical composition of the commercial carbon steel saws. Note that type 2 steel contains a higher content of vanadium, chromium and manganese. The addition of these elements increases the corrosion resistance of steel[35]. The carbon and sulfur composition of the samples was determined by combustion analysis, as indicated in Table 2.

The saws were cut into 25 x 4 mm (type 1) and into 25 x 6 mm pieces (type 2), which were then degreased in ultrasonic baths with detergent and alcohol. After they were dried, the samples were placed in a plasma processing system. This system allows for the deposition of films by plasma enhanced chemical vapor deposition (PECVD), the cleaning of surfaces by physical or chemical ablation, and plasma treatment of materials. The plasma processing system is illustrated schematically in Fig. 1.

Basically, the system consists of a cylindrical glass chamber with a useful volume of about 2 liters. Its

Table 2 — Carbon and sulfur composition of the carbon steel samples.

| | %C | %S |
|---|---|---|
| Type 1 steel | 0.7209 | 0.03358 |
| Type 2 steel | 0.5925 | 0.02252 |

Table 1 — Percentage composition of the chemical constituents of the carbon steel samples.

| | Al | Si | P | V | Cr | Mn | Ni | Cu | Mo | W |
|---|---|---|---|---|---|---|---|---|---|---|
| Type 1 steel | 0.2052 | 0.1690 | 0.0252 | 0.00231 | 0.2027 | 0.6942 | 0.0183 | 0.00449 | 0.0114 | 0.101 |
| Type 2 steel | 0.241 | 0.189 | 0.0305 | 0.101 | 1.168 | 0.999 | 0.0274 | 0.0302 | 0.0092 | 0.085 |

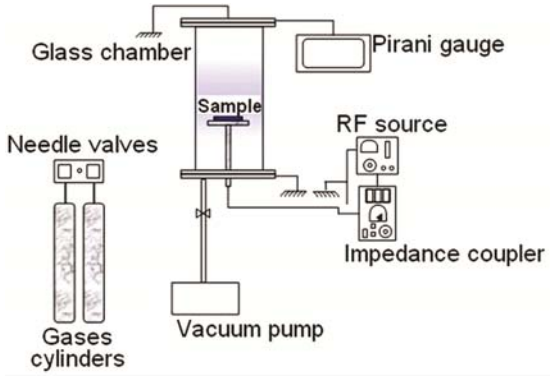


Fig. 1 — Experimental system employed to deposit hydrogenated amorphous carbon films on wood cutting saws.

ends are sealed with aluminum flanges which have openings for the entry of gas lines, meters and a vacuum pump. The chamber contains a stainless steel electrode through which the discharge is excited and which is also used as a sample holder. The aluminum flanges are normally grounded. The reactor is evacuated by an Edwards E2M-1a rotary vane pump with a pumping capacity of 18 $m^3$/h. The introduction of gases into the chamber is controlled by Edwards FCV10K extra fine needle valves, and the pressure inside the reactor is monitored with an Edwards APG-L Active Pirani gauge.

A 13.56 MHz radio frequency (RF) source (Tokyo Hy-Power, RF-300) is used for plasma excitation. Power transmission from the generator to the discharge is optimized by an impedance coupler (Tokyo Hy-Power, MB-300) composed of variable capacitors and inductors. Figure 2 shows a photograph of the system utilized in this study. The films investigated in this study were deposited from RF plasma (13.56 MHz) of acetylene and argon mixtures. The proportion of Ar was varied from 63 to 78% while that of acetylene was reduce in the same proportion in order to keep the total pressure of the gases at 1.8 Pa. The base pressure in the reactor, which is not included in the above value, was 0.73 Pa. The deposition time was 3600 s and the power of the excitation signal was 70 W. Before deposition, the samples were sputter cleaned with argon plasma (50 W, 19.27 Pa) for 180 s. Table 3 describes the conditions used in the deposition of the plasma films.

Measurements by electrochemical impedance spectroscopy (EIS) and polarization spectroscopy were carried out in a solution of 1 gram of NaCl per liter of water, to which $H_2SO_4$ was added until the pH of the solution reached a value of 3.5. The size

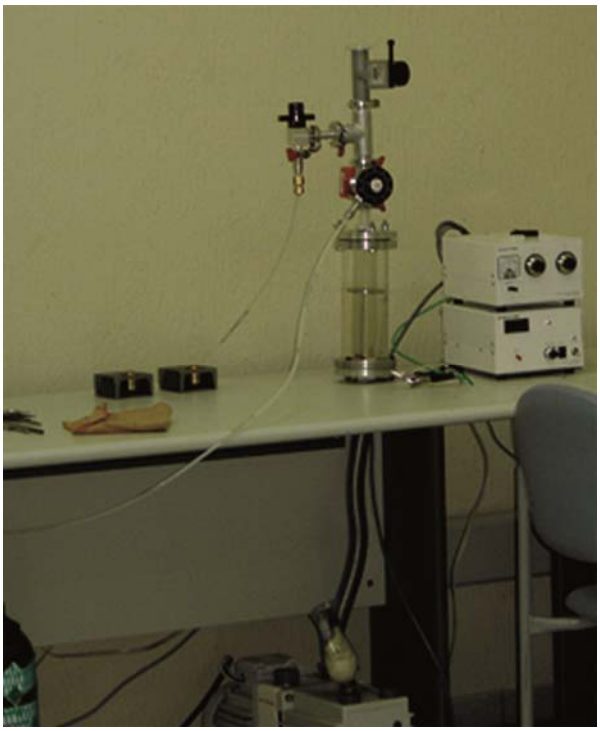

Fig. 2 — Photograph of the system depicted schematically in Figure 1.

Table 3 — Conditions for plasma film deposition.

| Process | Ar (%) | $C_2H_2$ (%) | Time (seconds) |
|---|---|---|---|
| 1 | 63 | 37 | 3,600 |
| 2 | 78 | 22 | 3,600 |

of the analyzed area of the type 2 samples was 0.5 cm x 1.0 cm, while that of type 1 was 1.0 cm x 0.4 cm.A reference electrode of saturated calomel and a counter electrode of platinum were used. The voltage amplitude applied was 10 mV. A frequency response analyzer (Solartron Analytical) was connected to a PAR-273A potentiostat. The electrochemical impedance was analyzed in a frequency range of $10^{-2}$ to $10^4$ Hz.

Potentiodynamic polarization tests were performed at a scan rate of 2 mV/s, beginning with a potential of – 900 mV and ending with a potential of – 300 mV. Polarization measurements were taken after the impedance analyses were concluded. Before starting the polarization tests, samples were immersed in corrosion solution for 10 minutes to stabilize the corrosion potential. The plasma-coated samples were placed in a scanning electron microscope (SEM) (Jeol JXA 840A) and subjected to secondary electron analysis to obtain a surface image of the films after the polarization tests.

## 3. Results and Discussion

### 3.1 EIS analysis of the samples

Figure 3 and 4 present the modulus of impedance vs. frequency curves and phase angle vs. frequency curves of the plasma-coated and non-coated samples.

As can be seen in Figs 3 and 4, the plasma deposition process with 78% of Ar increased the modulus of impedance of type 1 and 2 steel. The modulus of impedance curve (at 0.1 Hz) indicates that the two types of non-coated steel showed the same Z maximum. Some authors report the importance of the maximum Z value at low frequencies to characterize the resistance of a coating[36]. Z has a maximum value on type 2 steel with 78% of Ar, indicating greater resistance of the plasma film with 78% Ar presented at Fig. 4. According to the Bode diagram illustrated in Fig. 3, the phase angle of type 1 samples treated with 78% of Ar is practically double that of the sample with 63% of Ar. This increase in the phase angle indicates the greater corrosion protection afforded by the coating. An analysis of the phase angle of the coating samples deposited on the type 2 commercial steel saw (see Fig. 4) indicates that this angle did not undergo as significant a change as that of the type 1 steel sample (see Fig. 3). Figs 5 and 6 show the Nyquist curves obtained by the technique of electrochemical impedance spectroscopy.

In Fig. 5, the capacitive arc of the type 2 steel is larger than the arc of the type 1 steel. The larger capacitive arc indicates better corrosion resistance properties in attack solution. Figure 6 shows the curves of samples non-coated and coated with plasma film. Curves of coated samples have larger capacitive arcs compared to the samples of type 1 and 2 steel without film. The coating of 78% Ar presents the largest capacitive arc on both types of steel. The most appropriated circuit for the curves of EIS measurements was the Randle equivalent circuit. This circuit involving solution resistance ($R_{sol}$), charge transfer resistance ($R_{ct}$), and double layer capacitance ($C_{dl}$) is shown in Fig. 7. This equivalent circuit was suggested according to other works of plasma on steel[37–39].

$R_{sol}$ is the solution resistance which appears between the reference electrode and the sample, $C_{dl}$ is the double layer capacitance formed between the sample and the corrosion solution, $R_{ct}$ is the charge transfer resistance due to the process of electrochemical reaction. As greater charge transfer resistance smaller corrosive process. The roughness

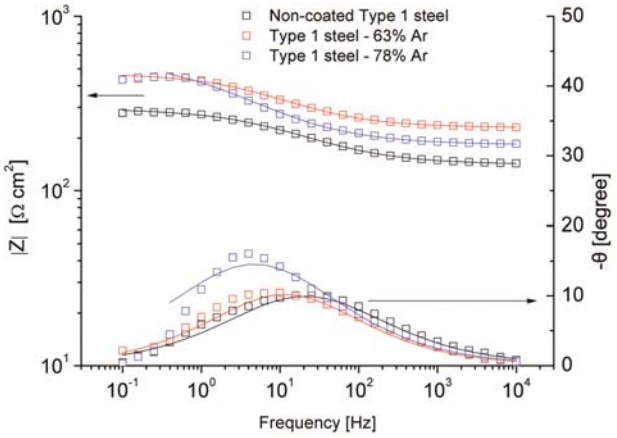


Fig. 3 — Modulus of Impedance versus Frequency and Phase Angle versus Frequency curves of the type 1 steel saw samples.

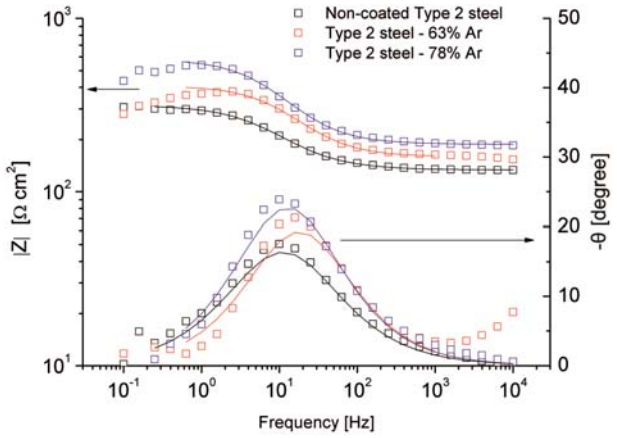


Fig. 4 — Modulus of Impedance versus Frequency and Phase Angle versus Frequency curves of the type 2 steel saw samples.

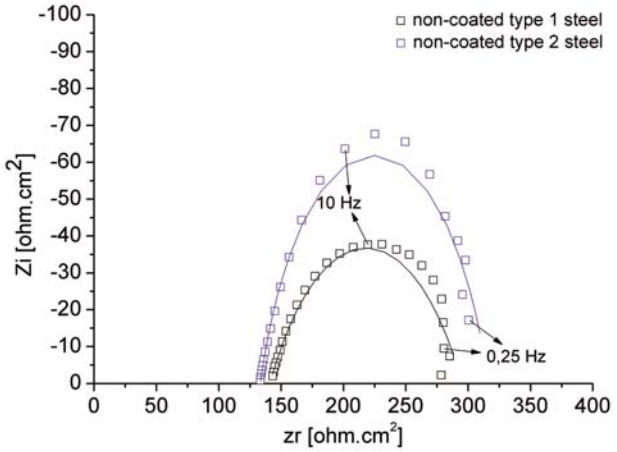


Fig. 5 — Nyquist curves of type 1 and 2 steel without film.

and heterogeneities of analyzed area make the capacitor becomes non-ideal, and capacitor changes to constant phase element ($Y_0$)[39].

The impedance of constant phase element is obtained by: $Z=1/[Y_0(j\omega)^n]$

where $Y_0$ is the constant phase element, ω is the angular frequency, n is a parameter to show whether CPE is close to ideal capacitor. For n=1, capacitor is ideal; for n=0 is a resistor; for n=-1 is an inductor[39,40].

Table 4 lists the value of each element of the Randle equivalent circuit obtained by adjustment of the EIS experimental curve.

The R1 values are due mainly to the contribution of the electrolyte used in the analysis. Note the increase in R1 after the deposition of the films, which indicates that the deposited film affords some protection. The R2 value tends to increase when the saw is coated with the film. In general, for both types of steel, this increase is more marked in the film deposited with a higher proportion of argon in the discharge.

The capacitance was calculated using the equation 1:

$$C = Y_o(\omega_{max})^{n-1} \quad \ldots (1)$$

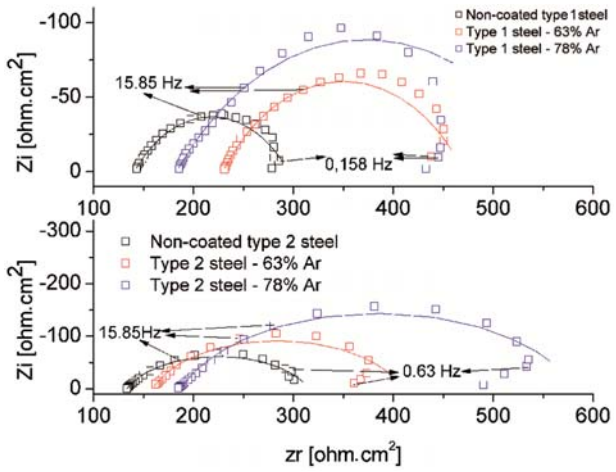


Fig. 6 — Nyquist curves of coated and uncoated samples of type 1 and 2 steel.

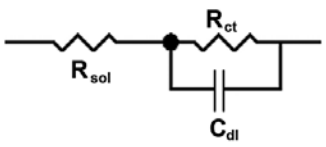


Fig. 7 — Equivalent circuit of plasma film on steel.

where $Y_o$ is the CPE value of the capacitance of the plasma film, and $\omega_{max}$ refers to the maximum value of the imaginary part of the frequency.

The plasma film thickness was calculated by using the equation below:

$$C = \varepsilon\varepsilon_o \frac{A}{d} \quad \ldots (2)$$

where C represents the capacitance of the plasma film, A is the exposed area of the sample, d is the thickness of the plasma film, $\varepsilon_o$ is the dielectric constant of free space 8.85 x $10^{-14}$ F/cm, and ε is the mean value of the dielectric constant of plasma 3.00[41]. Table 5 summaries the results of plasma film thickness calculated from the equation 2.

According to the calculation of the plasma layer thickness, calculated from the equation 2, all the samples presented thin film. The thickest films were over type 2 steel, which also has the best qualities of resistance to corrosion. Table 4 shows the n values of type 2 steel which are closer to an ideal capacitance and contributed to a higher film thickness. The same processes were applied on different substrates, and it must be considered the very thin layer of plasma over the substrate may interfere in the results. Indeed, the differences in the corrosion resistance can be ascribed to the initial properties of the substrate.

The dielectric constant of the plasma film adopted here was the mean value found in the work of Louh, who used a mixture of 100 to 200 sccm of *para*-xylene and argon gas for carbon deposition[41]. Because the film thickness is in the nanometric scale, capacitance of the coatings presented a higher value.

Table 5 — Thicknesses of plasma film obtained from the equation 2.

| Sample | C (F.cm$^{-2}$) | A (cm$^2$) | Thickness (nm) |
|---|---|---|---|
| 63% Ar-Type 1 steel | 2.65 x $10^{-4}$ | 0.4 | 0.40 |
| 78% Ar-Type 1 steel | 4.58 x $10^{-4}$ | 0.4 | 0.23 |
| 63% Ar-Type 2 steel | 9.06 x $10^{-5}$ | 0.5 | 1.46 |
| 78% Ar-Type 2 steel | 9.15 x $10^{-5}$ | 0.5 | 1.45 |

Table 4 — EIS data obtained from the equivalent circuit.

| Sample | R1 (Ω.cm$^2$) | $Y_o$ ($s^n.\Omega^{-1}.cm^{-2}$) | $\omega_{max}$ (Hz) | n | R2 (Ω.cm$^2$) | C (F.cm$^{-2}$) | Chi$^2$ |
|---|---|---|---|---|---|---|---|
| Type 1 steel as received | 141.1 | 5.90 x $10^{-4}$ | 6.310 | 0.567 | 154.0 | 2.66 x $10^{-4}$ | 13.07 x $10^{-4}$ |
| 63% Ar | 229.6 | 4.65 x $10^{-4}$ | 3.981 | 0.594 | 241.0 | 2.65 x $10^{-4}$ | 28.14 x $10^{-4}$ |
| 78% Ar | 183.1 | 6. 89 x $10^{-4}$ | 2.512 | 0.556 | 380.0 | 4.58 x $10^{-4}$ | 34.81 x $10^{-4}$ |
| Type 2 steel as received | 133.4 | 3.35 x $10^{-4}$ | 6.310 | 0.758 | 182.7 | 2.15 x $10^{-4}$ | 23.72 x $10^{-4}$ |
| 63% Ar | 159.0 | 1.42 x $10^{-4}$ | 10.00 | 0.805 | 250.3 | 9.06 x $10^{-5}$ | 63.30 x $10^{-4}$ |
| 78% Ar | 187.6 | 1.32 x $10^{-4}$ | 6.310 | 0.801 | 394.9 | 9.15 x $10^{-5}$ | 33.41 x $10^{-4}$ |

In the work of Barranco, which involved a study of the treatment of trimethylsilane plasma, a thickness of 57 nm was obtained. For these samples, capacitances of the order of 6.40 x $10^{-8}$ F/cm$^2$ were reported[42]. This information found in the literature is consistent with that found in this work, where the high capacitance is linked to the low thickness, while in the work of Barranco the lowest capacitance is associated with a higher film thickness. Lastly, it should be considered that the corrosion resistance results are compatible with the polymeric nature of the films, which were characterized in a previous paper.[20]

### 3.2 Analysis of the polarization curves of the steel samples

Figure 8 illustrates the polarization curves of the non-coated type 1 and type 2 steel samples. Note that the type 2 steel, which contains higher contents of some alloying elements, presents a more noble corrosion potential. Sample type 1 has lower corrosion potential and higher corrosion density in anodic branch. Anodic current density is lower on sample non-coated type 2. This fact shows that sample type 2 has higher corrosion resistance.

The graph in Fig. 9 shows the polarization curves of the coated and non-coated type 2 steel saw samples. Note that the corrosion potential does not vary significantly, remaining at about - 0.66 V on the curves, which indicates that the chemical composition of the plasma has little effect on this parameter. The cathodic process is approximately between -0,8 to -0,66V, and anodic process is around -0,66 to -0,33V.

An analysis of the polarization curves of the type 1 steel sample (Fig. 10) indicates that the corrosion potential remained practically constant. Therefore, the corrosion potential of both type 1 and type 2 steel did no change significantly in response to the plasma-deposited film.

Table 6 lists the parameters obtained from the polarization curves, which correspond to the corrosion potential ($E_{corr}$) and the corrosion current density ($i_{corr}$). The corrosion current density or corrosion rate was determined by the Tafel extrapolation method.

An analysis of the data in Table 5 indicates that both type 1 and type 2 steel samples decreased slightly in corrosion current density after the deposition of the films.

The results of the films deposited on the two types of steel do not show a noticeable difference in corrosion current density under the two conditions of film deposition. The corrosion rate of the plasma film of 78% of argon showed lower value on the two types

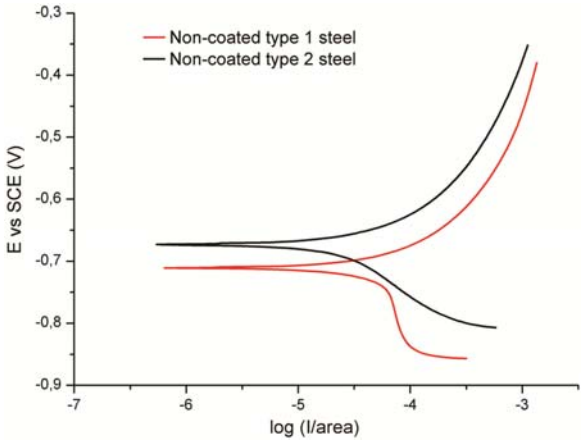


Fig. 8 — Polarization curves of non-coated steel saws.

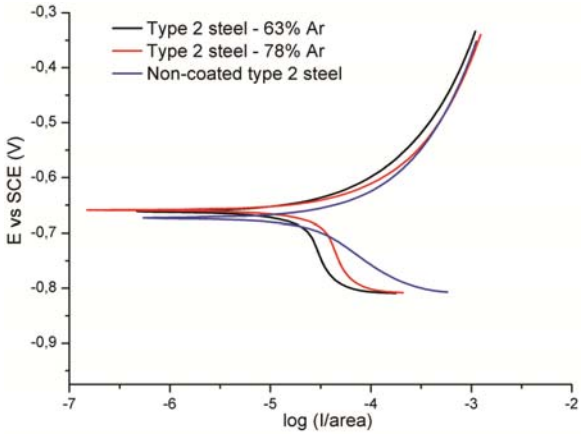


Fig. 9 — Polarization curves of type 2 steel samples with and without film coatings deposited in mixed acetylene and argon plasmas containing different proportions of the compound in the mixture.

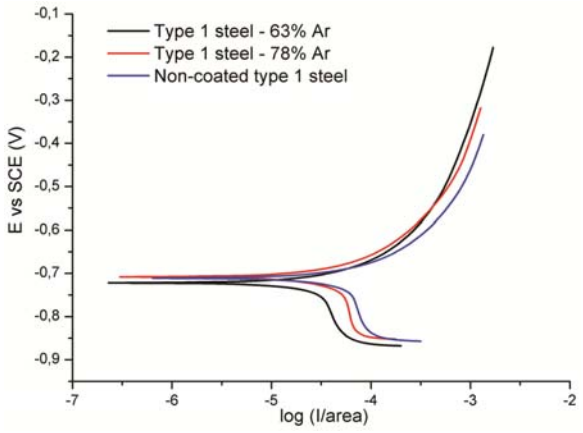


Fig. 10 — Polarization curves of the type 1 steel with and without plasma treatment.

of steel, probably due to the fact that the argon content varied by only 15% from one sample to the other. However, the effectiveness of $E_{corr}$ of the type 2

Table 6 — Corrosion parameters obtained in the polarization tests.

| Sample | $E_{corr}$ (mV X SCE) | $i_{corr}$ ($\mu A/cm^2$) |
|---|---|---|
| Type 1 steel saw | | |
| Without coating film | -0.71 | $29.00 \times 10^{-6}$ |
| 63% Ar | -0.72 | $15.00 \times 10^{-6}$ |
| 78% Ar | -0.71 | $9.00 \times 10^{-6}$ |
| Type 2 steel saw | | |
| Without coating film | -0.68 | $15.00 \times 10^{-6}$ |
| 63% Ar | -0.66 | $9.00 \times 10^{-6}$ |
| 78% Ar | -0.66 | $5.00 \times 10^{-6}$ |

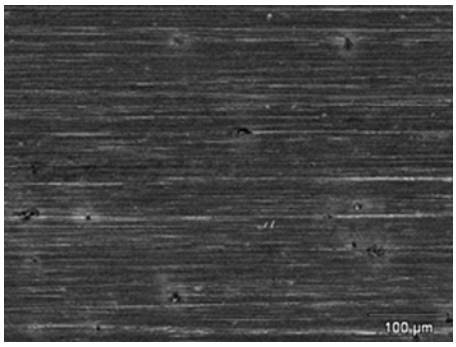


Fig. 11 — SEM micrograph of type 1 steel without plasma coating.


Fig. 12 — SEM micrograph of type 1 steel plasma coated under condition 1 (63% Ar).

steel samples was greater, since these samples contained higher contents of alloying elements.

### 3.3 SEM analysis of the steel saw samples

Commercial type 1 and type 2 steel saws as-received were not immersed in corrosion solution. After the corrosion tests in attack solution, the commercial type 1 and type 2 steel saws, plasma film-coated, were analyzed by scanning electron microscopy (SEM); Figs 9-14 shows the results of these analyses.

The non-coated samples (Figures 11 and 14) show the surface characteristics resulting from the steel machining process. In samples of type 2 steel can be seen cavity regions. The images of figures coated with plasma (Figs 12, 13, 15, 16) indicate the absence of

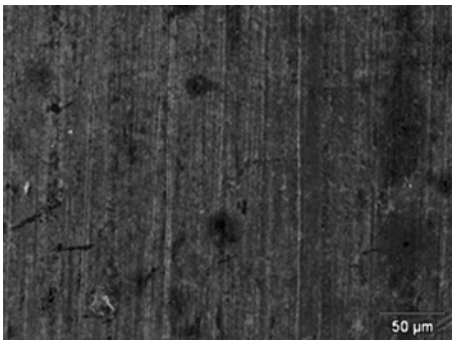


Fig. 13 — SEM micrograph of type 1 steel plasma coated under condition 2 (78% Ar).

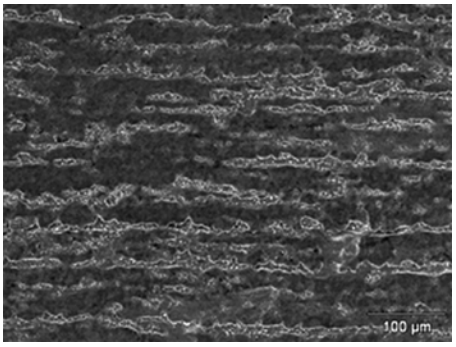


Fig. 14 — SEM micrograph of type 2 steel without plasma coating.

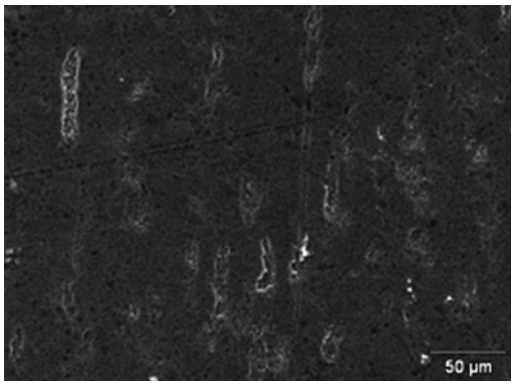


Fig. 15 — SEM micrograph of type 2 steel plasma coated under condition 1 (63% Ar).

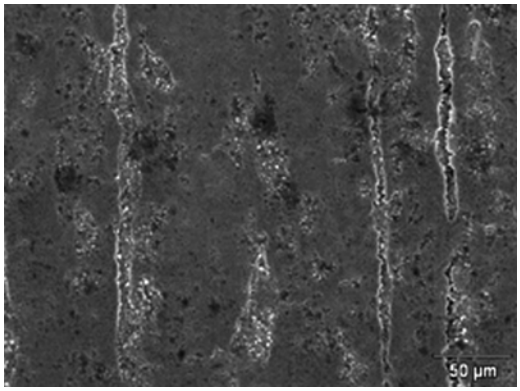


Fig. 16 — SEM micrograph of type 2 steel plasma coated under condition 2 (78% Ar).

localized corrosion. The images corroborate with the corrosion tests where there is no significative corrosive attack on coated samples.

## 4 Conclusions

The impedance spectroscopy results led to the conclusion that the plasma-deposited film increased the corrosion resistance of the samples of both type 1 and type 2 steel. The polarization curves indicate that the plasma treatment of the two types of steel reduced the corrosion current density of the coated saws. The SEM micrographs did not exhibit corrosion typical of a polarization test in the plasma-coated samples because the thickness of plasma-deposited film was very thin.

Lastly, it can be stated that the deposition of the polymeric film yielded benefits in terms of protecting the carbon steel. Moreover, the response of the system to corrosion attack depends not only on the chemical composition of the plasma but also on the base material of the cutting tool.

The change in the corrosion resistance of the plasma film, based on the high capacitance values, is due to the following factors: The small thickness of the plasma layer, which allows for the passage of ionic species (due to its more permeable porous structure), the film's chemical inertness decreases over time in the corrosive environment, and the film's roughness accelerates the corrosion process, making the layer less protective.

## References


1 Kaminski J, Rudnicki J, Nouveau C, Savan A & Beer P, *Surf Coatings Technol*, 200 (2005) 83.
2 da Cruz N. C, Rangel E C, Wang J, Trasferetti B C, Davanzo C U, Castro S G C & de Moraes M A B, *Surf CoatingsTechnol*, 126 (2000)123.
3 Durrant S F, Rangel E C, da Cruz N C, Castro S G C & Bica de Moraes M A, *Surf Coatings Technol*, 86 (1996) 443.
4 Rangel E C, Da Cruz N C, Kayama M E, Rangel R C C, Marins N & Durrant S F, *Plasmas Polym*, 9 (2004) 1.
5 Yasuda H, Yu Q & Chen M, *Prog Org Coatings*, 41(2001) 273.
6 Bruno G, Capezzuto P, Cramarossa F & D'Agostino R, *ThinSolidFilms*, 67 (1980) 103.
7 Jeng Y R, Islam S, Wu K T, Erdemir A &Eryilmaz O, *J Mech*, 33 (2017) 769.
8 Jedrzejczak A, Batory D, Dominik M, Smietana M, Cichomski M, Szymanski W, Bystrzycka E, Prowizor M, Kozlowski W & Dudek M, *Surf Coatings Technol*, 329 (2017) 212.
9 Yasuda H K, *Plasma Polymerization*, Academic Press, ISBN: 9780323139458, (1985).
10 Ganji J, Kosarian A & Kaabi H, *Silicon*, 12 (2020) 723.
11 Morita S & Hattori S, in *Plasma Deposition, Treatment and Etching of Polymers*, edited by D'Agostino R (Academic Press), ISBN: 9780323139083,(1990).
12 Shi F F, *Surf Coatings Technol*, 82 (1996) 1.
13 Biederman H &Osada Y, *Plasma Polymerization Processes*, Elsevier Science, ISBN: 9780444887245, (1992).
14 Tibbitt J M, Shen M & Bell A T, *J Macromol Sci Part A – Chem*, 10 (1976) 1623.
15 Tkacz-Śmiech K, Dyndał K, Sanetra J & Jaglarz J, *Vacuum*, 146 (2017) 15.
16 Constantinou M, Pervolaraki M, Koutsokeras L, Prouskas C, Patsalas P, Kelires P, Giapintzakis J &Constantinides G, *Surf Coatings Technol*, 330 (2017) 185.
17 Robertson J, *Mater SciEng R Reports*, 37 (2002) 129.
18 Kuo S C, Kunhardt E E & Srivatsa A R, *Appl Phys Lett*, 59 (1991) 2532.
19 Pastel P W &Varhue W J, *J Vac Sci Technol A*, 9 (1991) 1129.
20 Rangel E C, de Souza E S, de Moraes F S, Marins N M S, Schreiner W H, & Cruz N C, *Thin Solid Films*, 518 (2010) 2750.
21 Treutler C P O, *Surf Coatings Technol*, 200 (2005) 1969.
22 Robertson J, *Thin Solid Films*, 383 (2001) 81.
23 Metin S, Kaufman J H, Saperstein D D, Scott J C, Heyman J, Haller E E, *J Mater Res*, 9 (1994) 396.
24 Kobayashi S, Ohgoe Y, Ozeki K, Sato K, Sumiya T, Hirakuri K K& Aoki H, *DiamRelat Mater*, 14 (2005) 1094.
25 Maguire P D, McLaughlin J A, Okpalugo T I T, Lemoine P, Papakonstantinou P, McAdams E T, Needham M, Ogwu A A, Ball M & Abbas G A, *DiamRelat Mater*, 14 (2005) 1277.
26 Dahm K L &Dearnley P A, *Wear*, 259 (2005) 933.
27 Butter R, Allen M, Chandra L, Lettington A H & Rushton N, *DiamRelat Mater*, 4 (1995) 857.
28 Rismani E, Yeo R, Sinha S K, Yang H & Bhatia C S, *Tribol Lett*, 50 (2013) 233.
29 Pathem B K, Guo X C, Rose F, Wang N, Komvopoulos K, Schreck E, Marchon B, *IEEE Trans Magn*, 49 (2013) 3721.
30 Yeh R H, Chao T M &Tan A H, *J MagnMagnMater*, 351 (2014) 76.
31 Mohammadinia E, Elahi S M &Shahidi S, *Mater Sci Semicond Process*, 74 (2018) 7.
32 Pillai R, Batra N, Manocha LM, Machinewala N, *Surf Interfaces*, 7 (2017) 113.
33 Pillai R, Jariwala C, Kumar K, Kumar S, *Surf. Interfaces*, 9 (2017) 21.
34 Moolsradoo N, Watanabe S, *Adv Mater SciEng*, 2017 (2017) 6.
35 Callister W D, *Materials Science and Engineering: An Introduction*, John Wiley and Sons, ISBN: 9781118324578, (2013).
36 Amirudin A & Thierry D, *Prog Org Coatings*, 26 (1995) 1.
37 Saadi C, Ozanam F, Coffinier Y, Gabler C, Brenner J, Boukherroub R, Medjram M S, Szunerits S, *Surf Coatings Technol*, 206 (2012) 3626.
38 Jing W, Guichang L & Jun X, *Plasma Sci Technol*, 12 (2010) 461.
39 Li D, Guruvenket S, Azzi M, Szpunar J A, Klemberg-Sapieha J E, Martinu L, *Surf Coatings Technol*, 204 (2010) 1616.
40 Jorcin J B, Orazem M E, Pébère N &Tribollet B, *Electrochim Acta*, 51 (2006) 1473.
41 Louh S P, Leu I C &Hon M H, *Diam Relat Mater*, 14 (2005) 1005.
42 Barranco V, Thiemann P, Yasuda H K, Stratmann M & Grundmeier G, *Appl Surf Sci*, 229 (2004) 87.